

# A New Nanohybrid Photocatalyst between Anatase (TiO<sub>2</sub>) and Layered Titanate

Hyun-Cheol Lee, Hyun Jung, Jae-Min Oh, and Jin-Ho Choy\*

National Nanohybrid Materials Laboratory, School of Chemistry and Molecular Engineering,  
Seoul National University, Seoul 151-747, Korea

Received October 9, 2001

A new microporous TiO<sub>2</sub>-pillared layered titanate has been successfully prepared by hybridizing the exfoliated titanate with the anatase TiO<sub>2</sub> nano-sol. According to the X-ray diffraction analysis and N<sub>2</sub> adsorption-desorption isotherms, the TiO<sub>2</sub>-pillared layered titanate showed a pillar height of ~2 nm with a high surface area of ~460 m<sup>2</sup>/g and a pore size of ~0.95 nm, indicating that a microporous pillar structure is formed. Its photocatalytic activity was evaluated by measuring the photodegradation rate of 4-chlorophenol during irradiation of catalyst suspensions in an aqueous solution. An enhancement in activity of ca. 170% was obtained for TiO<sub>2</sub>-pillared layered titanate compared to that of the pristine compound such as layered cesium titanate.

**Keywords :** TiO<sub>2</sub>-pillared titanate, Anatase, Photocatalyst, Porous materials.

## Introduction

The pillaring of layered compounds by inorganic molecular clusters or nano-sols offers a promising means of fabricating porous materials with zeolitic properties.<sup>1-5</sup> In particular, the semiconductor nano-sol pillars have attracted special attention due to their excellent photocatalytic activity. As reported previously,<sup>6-8</sup> the pillared semiconducting anatase TiO<sub>2</sub> gives rise to a remarkable enhancement in photocatalytic activity compared to unsupported catalysts. Such photocatalytic activity of semiconductor pillars is also known to be dependent on the type of host layer. For example, CdS-ZnS pillar stabilized in the interlayer space of a layered semiconductor shows much higher photoactivity than that pillared in an insulating host lattice, since electron and hole recombination is effectively suppressed due to electron transfer between guest and host.<sup>7,8</sup>

Generally, it is not easy to stabilize a semiconducting pillar like TiO<sub>2</sub> in layered transition metal oxides such as titanate and titanoniobate since these types of host materials exhibit no swelling ability. This is explicable as a result of the high layer charge of the host lattice which hinders an effective intercalation of TiO<sub>2</sub> sol particles since the interlayer space of the host layer does not undergo sufficient swelling to permit large guest species to be intercalated. In light of this, we have developed a novel route for generating a well-ordered TiO<sub>2</sub>-pillared layered titanate with an enhanced photocatalytic activity, which could only be realized by one notable step, namely the exfoliation of host titanate lattice and its restacking in the presence of well-developed anatase TiO<sub>2</sub> nano-sol.<sup>9</sup> Such a hybridization between exfoliated titanate and anatase TiO<sub>2</sub> nano-sol at the molecular level is found to be advantageous for the preparation of porous structured material, since it provides a way of accessing guest species freely into the interlayer space of the host lattice without any steric hindrance.<sup>10-13</sup>

## Experimental Procedures

**Sample preparation.** The pristine cesium titanate (Cs<sub>0.67</sub>Ti<sub>1.83</sub>□<sub>0.17</sub>O<sub>4</sub>, □ express vacancy) was prepared by heating a stoichiometric mixture of Cs<sub>2</sub>CO<sub>3</sub> and TiO<sub>2</sub> at 800 °C for 20 h.<sup>14</sup> The corresponding protonic form, H<sub>0.67</sub>Ti<sub>1.83</sub>□<sub>0.17</sub>O<sub>4</sub> · H<sub>2</sub>O, was obtained by reacting the cesium titanate powder with 1 M HCl aqueous solution at room temperature for 3 days. During the proton exchange reaction, the HCl solution was replaced with a fresh one everyday.<sup>15</sup> The layered proton-type titanate was exfoliated into single titanate sheets by intercalating TBA (tetra-butylamine) molecules, as reported previously.<sup>16</sup> On the other hand, the mono-dispersed and non-aggregated TiO<sub>2</sub> nano-sol was prepared by adding dropwise titanium isopropoxide (30 mL) with acetylacetone (20.38 mL) to 0.015 M HNO<sub>3</sub> aqueous solution (180 mL) under vigorous stirring, and then by peptizing at 60 °C for 8 h.<sup>17</sup> A TiO<sub>2</sub>-pillared layered titanate was prepared by hybridizing the exfoliated titanate sheets with the TiO<sub>2</sub> nano-sol particles at 60 °C for 24 h. The resulting powder was collected by centrifuging (12,000 rpm, 10 min), washed with a mixed solution of distilled water and ethanol (1 : 1, v/v) to remove excess TiO<sub>2</sub> sol, and then dried in an ambient atmosphere. Finally, the obtained material was heated at 300 °C for 2 h in order to complete the pillaring process.

**Sample characterization.** The crystal structures of the pristine titanate and its derivatives were studied by powder X-ray diffraction (XRD) measurements using Ni-filtered Cu-K $\alpha$  radiation ( $\lambda = 1.54056 \text{ \AA}$ ) with a graphite diffracted beam monochromator, and their chemical compositions were determined by performing elemental analysis (ICP & CHNS). The ICP results indicate that 0.67 mol of cesium ions is incorporated into the crystal lattice, and cesium ions are successfully exchanged with protons by acid treatment. Thermogravimetric analysis (TGA) was also carried out to check the thermal stability of the TiO<sub>2</sub>-intercalated titanate in an ambient atmosphere where the heating rate was fixed at 5 °C/min. To determine the surface area and porosity of the sam-

\*To whom all correspondences should be addressed. Tel: +82-2-880-6658; Fax: +82-2-872-9864; e-mail: jhchoy@plaza.snu.ac.kr

ples, nitrogen adsorption-desorption isotherms were measured volumetrically at liquid nitrogen temperature with a homemade computer-controlled measurement system.<sup>2</sup> UV-vis spectra measurements were performed to evaluate the photo-chemical properties of the samples. The band gap energies were determined from the onset of the diffuse reflectance spectra, which were obtained in a magnitude proportional to the extinction coefficient ( $\kappa$ ) through the Kubelka-Munk function.<sup>18</sup>

**Photocatalytic reaction.** The photocatalyst (10 mg) was dispersed in a quartz cell with 100 mL of 4-chlorophenol solution ( $10^{-4}$  M), which was vigorously stirred under oxygen gas bubbling conditions. One side of the cell was irradiated with UV-vis light from a 300 W Xe lamp at room temperature. The photocatalytic activity of the samples was evaluated by measuring the photodegradation rate of 4-chlorophenol in an aqueous solution. UV-vis absorption spectra were recorded on a Perkin-Elmer Lambda 12 spectrometer equipped with an integrating sphere of 60 nm in diameter using BaSO<sub>4</sub> as a standard.

### Results and Discussion

The XRD patterns of the pristine layered cesium titanate and its protonated derivative were found to be well-indexed on the basis of lepidocrocite structure with orthorhombic symmetry. Figure 1 represents the XRD patterns of the selected samples under the pillaring process. From the (020) reflection at  $2\theta = 10.28^\circ$  (Figure 1a), a basal spacing of 0.86 nm for the proton-type layered titanate can be determined. Upon acid treatment, the (020) reflection shifts toward a lower angle ( $2\theta = 9.6^\circ$ ), indicating a lattice expansion (0.92

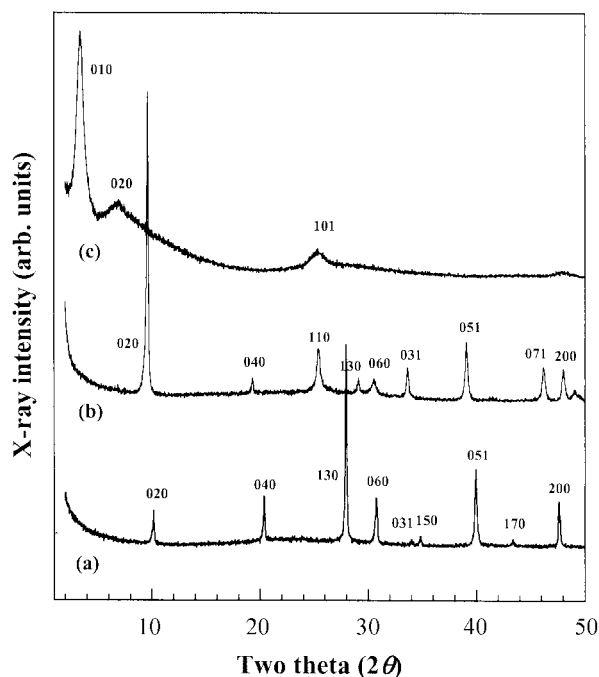


**Figure 1.** Powder XRD patterns of layered cesium titanate (a), acid-treated sample (b), and TiO<sub>2</sub>-pillared layered titanate with heat treatment at 300 °C (c).

nm) due to the intercalation of water molecules into the interlayer space of the layered titanate (Figure 1b). Before the ion-exchange reaction with TiO<sub>2</sub> nano-sol, the proton-type layered titanate was exfoliated by intercalating tetrabutylamine molecules. The exfoliated titanate does not show any basal reflections, indicating that the titanate single sheets are dispersed in an aqueous medium.<sup>19</sup> Upon reaction of the exfoliated titanate with anatase TiO<sub>2</sub> nano-sol, the (020) reflection of the proton-type phase is displaced to the (010) reflection of the restacked titanate at a lower angle ( $2\theta = 2.1^\circ$ ,  $d = 4.36$  nm), suggesting that the mono-dispersed TiO<sub>2</sub> nano-sol is stabilized in the interlayer space of titanate. The well-developed (010) peaks at  $2\theta = 2.1^\circ$ ,  $4.2^\circ$ , and  $6.3^\circ$  indicate that the resulting TiO<sub>2</sub>-pillared titanate is fairly well ordered along the b-axis. After calcinating at 300 °C for 2 h, its basal spacing decreases to 2.56 nm (Figure 1c), which is mainly attributed to the dehydroxylation of pillared TiO<sub>2</sub> nano-sol particles and to the pyrolysis of acetylaceton molecules coordinated to the surface of TiO<sub>2</sub> nano-sol. Such a pillared structure is maintained even after calcinating at 350 °C for 2 h, whereas it becomes collapsed to an amorphous phase above 400 °C. It is worthwhile to mention here that the thermal stability of layered titanate is significantly enhanced by pillaring the TiO<sub>2</sub> sol particles due to the formation of strong chemical bonds between the TiO<sub>2</sub> nanoparticles and the layered titanate lattice in the interlayer space.

According to the CHNS analysis, no trace of nitrogen was detected for the TiO<sub>2</sub>-intercalated layered titanate prepared by hybridizing the exfoliated titanate with TiO<sub>2</sub> nano-sols, indicating that the tetrabutylamine molecules in the interlayer of titanate was fully exchanged by TiO<sub>2</sub> nano-sols coordinated with acetylaceton. Therefore, the TiO<sub>2</sub>-intercalated layered titanate contains water and acetylaceton only in the interlayer space. Consequently, when the sample is heated at 300 °C for 2 h in air, acetylaceton molecules in the interlayer space could be removed since the boiling point of acetylaceton is known to be  $\sim 140.4$  °C.

Figure 2 represents the TG-DTG curve for the TiO<sub>2</sub>-intercalated layered titanate, and its weight loss is found to be extended over a wide temperature range due to the combination of several factors contributing to weight decrease such as dehydration, decomposition, and dehydroxylation. The first step up to  $\sim 120$  °C is certainly due to the dehydration of water in titanate layers, and the second step between 120 and 260 °C is attributed to the oxidative decomposition of acetylaceton in the interlayer surface of titanate. The third step beyond 280 °C is due to the dehydroxylation of the TiO<sub>2</sub> sol in the host layer. All these results coincide well with CHNS analysis data indicating that the tetrabutylamine molecules in the titanate layer are completely replaced with the TiO<sub>2</sub> nano-sol coordinated with acetylaceton during the hybridization procedure.

According to the nitrogen adsorption-desorption isotherm, the present TiO<sub>2</sub>-pillared layered titanate could be of the type I and/or IV in the BDDT classification, which is characteristic of microporous adsorbents.<sup>20</sup> In addition, the hy-

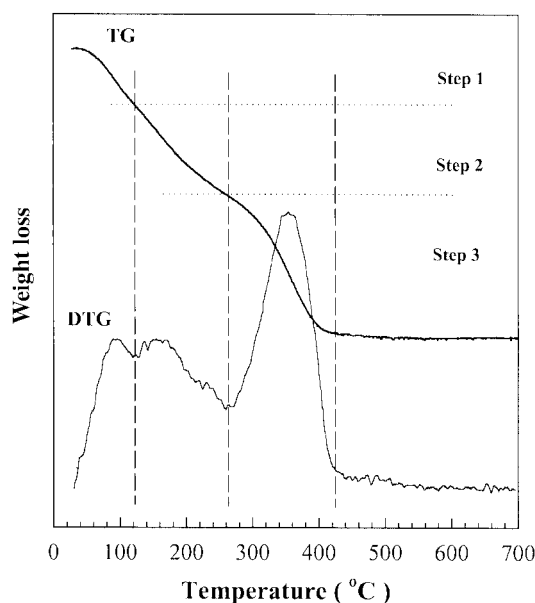


Figure 2. TG & DTG curves for TiO<sub>2</sub>-intercalated layered titanate.

steresis loop resembles H4 in the IUPAC classification, indicating the presence of open slit-shaped pores with fairly wide bodies and narrow short narrow necks (Figure 3).<sup>20</sup> Surprisingly, the surface area of the TiO<sub>2</sub>-pillared titanate is determined to be ~460 m<sup>2</sup>/g with a pore volume of 0.17 ml liquid nitrogen per gram of material, which enormously exceeds that of pristine layered cesium titanate (~1 m<sup>2</sup>/g), and is the largest among semiconducting nano-sol particles-pillared layered transition metal oxides so far reported. The pore size distribution curve has been calculated by using the

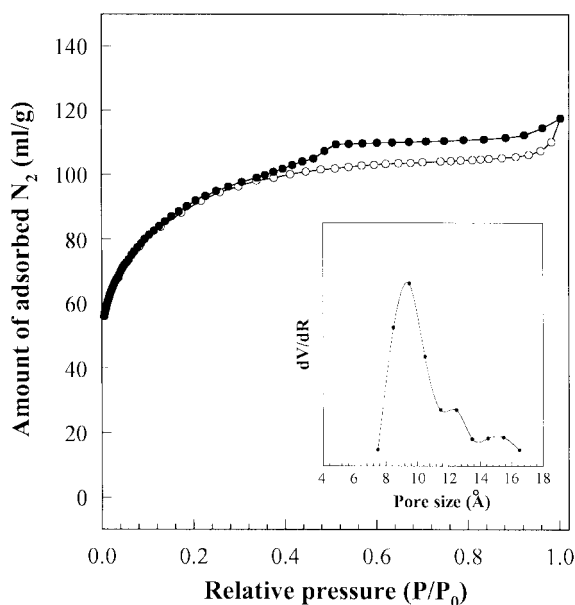


Figure 3. Nitrogen adsorption-desorption isotherms of TiO<sub>2</sub>-pillared layered titanate with heat-treatment at 300 °C (circles). The filled and open symbols represent adsorption and desorption data, respectively. The inset shows the pore size distribution curve for TiO<sub>2</sub>-pillared titanate.

Table 1. Specific surface areas, pore volumes and pore diameters of layered titanate and TiO<sub>2</sub>-pillared layered titanate

Sample identification	Surface area (m <sup>2</sup> /g)		Pore volume (ml/g)		Pore diameter (Å) <sup>b</sup>
	S <sub>BET</sub>	S <sub>Langmuir</sub>	V <sub>Total</sub> <sup>a</sup>	V <sub>micro</sub> <sup>b</sup>	
Layered cesium titanate	1	1	0	0	0
Proton-type layered titanate	13	24	0	0	0
Anatase-pillared layered titanate-300 °C	251 <sup>c</sup>	458 <sup>c</sup>	0.171	0.153	9.5

<sup>a</sup>Specific total pore volume at P/P<sub>0</sub> = 0.98. <sup>b</sup>Estimated by t-plot method. <sup>c</sup>The correlation coefficient (R = 0.9981) of S<sub>Langmuir</sub> is more close to ~1 than that (R = 0.9936) of S<sub>BET</sub>.

micropore analysis (MP) method, which reveals that the pores in the TiO<sub>2</sub>-pillared titanate mainly consist of micropores with a size of ~0.95 nm (inset of Figure 3).<sup>21</sup> The pore volumes and pore diameters for the pillaring process of layered titanate are summarized in Table 1.

Figure 4 shows the UV-vis diffuse reflectance spectrum of the TiO<sub>2</sub>-pillared layered titanate, which is compared with that of the pristine cesium titanate. Upon reacting the host titanate with the anatase TiO<sub>2</sub> nano-sol, the layered cesium titanate band (~3.5 eV) shifts to a longer wavelength region corresponding to a band gap energy of ~2.7 eV. This is attributed to a red shift in the onset of the spectra as a result of hybridizing the layered titanate with anatase TiO<sub>2</sub> nano-sol. Similar results have been reported for Fe<sub>2</sub>O<sub>3</sub>-pillared montmorillonite,<sup>22,23</sup> TiO<sub>2</sub>-pillared montmorillonite,<sup>24</sup> SiO<sub>2</sub>/TiO<sub>2</sub>-pillared montmorillonite,<sup>2</sup> and various CdS/ZnS-pillared layered compounds.<sup>6,25,26</sup>

The photocatalytic activity was evaluated by measuring

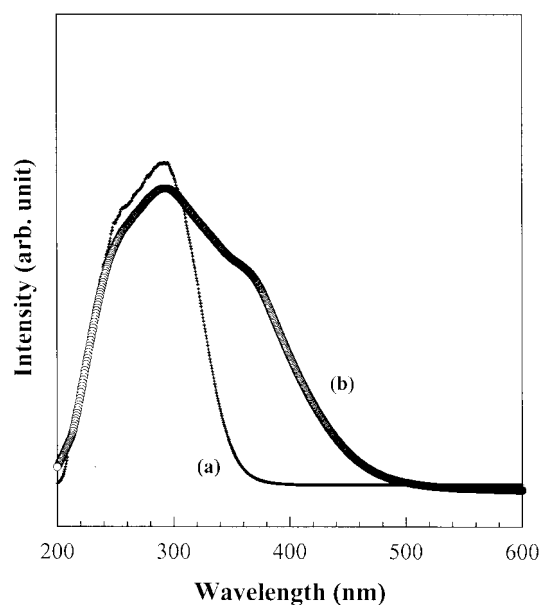
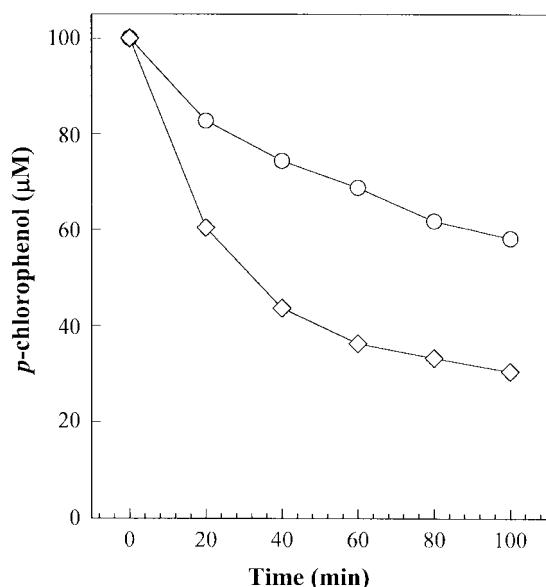


Figure 4. Diffuse UV-vis spectra for layered protonic titanate (a), and TiO<sub>2</sub>-pillared layered titanate (b).



**Figure 5.** Cumulative photocatalytic decomposition of 4-chlorophenol from 100 mL ( $10^{-4}$  M) solution in the presence of 10 mg catalysts (10 mg) under UV irradiation of 300 W Xe lamp. The circle and diamond symbols represent layered cesium titanate and  $\text{TiO}_2$ -pillared layered titanate, respectively.

the photodegradation rate of 4-chlorophenol during the irradiation on catalyst suspensions in an aqueous solution. Figure 5 represents the degradation rate of 4-chlorophenol by photocatalysts during 100 min. The photodegradation of the  $\text{TiO}_2$ -pillared layered titanate showed higher activity ( $0.695 \mu\text{mol min}^{-1}$ ) than that of the pristine layered titanate ( $0.4176 \mu\text{mol min}^{-1}$ ). An enhancement in activity by ca. 170% could be obtained for the  $\text{TiO}_2$ -pillared layered titanate compared to that of the pristine compound, which is attributed to the presence of the anatase  $\text{TiO}_2$  nano-sol in the interlayer space. The electron-hole recombination is effectively suppressed due to electron transfer between guest and host.<sup>27</sup>

### Conclusions

A new microporous  $\text{TiO}_2$ -pillared layered titanate was successfully prepared through an exfoliation-restacking route. The  $\text{TiO}_2$ -pillared layered titanate exhibited the highest surface area ( $460 \text{ m}^2/\text{g}$ ) with an excellent thermal stability up to  $350^\circ\text{C}$ , which is the last catalyst ever reported among semiconductor-pillared transition metal oxides.<sup>27,28</sup> According to the nitrogen adsorption isotherm measurement, the present pillared material consists of micropores in the main. Based on the above results, a model for multilayer-stacked interlayer sol particles is proposed in which the pillars between sol particles and titanate layers provide a unique micropore structure. A remarkable enhancement in photocatalytic activity by ca. 170% could be obtained for the  $\text{TiO}_2$ -pillared

layered titanate compared to that of the pristine compound by performing the photodegradation of 4-Chlorophenol.

**Acknowledgment.** This work was supported by the Korean Science and Engineering Foundation through the National Research Laboratory (NRL) project'99 and by the Korean Ministry of Education through the BK 21 fellowship and by the LG Electronics Institute of Technology.

### References

- Han, Y. S.; Choy, J. H. *J. Mater. Chem.* **1998**, *8*, 1459.
- Choy, J. H.; Park, J. H.; Yoon, J. B. *J. Phys. Chem. B* **1998**, *102*, 5991.
- Choy, J. H.; Kim, J. T.; Yoon, J. B.; Kim, D. K. *Mol. Cryst. Liq. Cryst.* **1998**, *311*, 315.
- Han, Y. S.; Yamanaka, S.; Choy, J. H. *J. Solid State Chem.* **1999**, *144*, 45.
- Han, Y. S.; Yamanaka, S.; Choy, J. H. *Appl. Catal. A* **1998**, *174*, 83.
- Sato, T.; Masaki, K.; Yoshioka, T.; Okuwaki, A. *J. Chem. Tech. Biotechnol.* **1993**, *58*, 315.
- Sato, T.; Yamamoto, Y.; Fujishiro, Y.; Uchida, S. *J. Chem. Soc., Faraday Trans.* **1996**, *92*, 5089.
- Uchida, S.; Yamamoto, Y.; Fujishiro, Y.; Watanabe, A.; Ito, O.; Sato, T. *J. Chem. Soc., Faraday Trans.* **1997**, *93*, 3229.
- Choy, J. H.; Lee, H. C.; Jung, H.; Hwang, S. J. *J. Mater. Chem.* **2001**, *11*, 2232.
- Bissessur, R.; Heising, J.; Hirpo, W.; Kanatzidis, M. *Chem. Mater.* **1996**, *8*, 318.
- Heising, J.; Bonhomme, F.; Kanatzidis, M. G. *J. Solid State Chem.* **1998**, *139*, 22.
- Wang, L.; Rocci, M.; Brazis, P.; Kannewurf, C. R.; Kim, Y. I.; Lee, W.; Choy, J. H.; Kanatzidis, M. G. *J. Am. Chem. Soc.* **2000**, *122*, 6629.
- Modestov, A.; Glezer, V.; Marjasin, I.; Lev, O. *J. Phys. Chem. B* **1997**, *101*, 4623.
- Grey, I. E.; Madsen, I. C.; Watts, J. A.; Bursill, L. A.; Kwiatkowska, J. *J. Solid State Chem.* **1985**, *58*, 350.
- Sasaki, T.; Komatsu, Y.; Fujiki, Y. *J. Chem. Soc., Chem. Commun.* **1991**, *817*, 2222.
- Sasaki, T.; Watanabe, M.; Hashizume, H.; Yamada, H.; Nakazawa, H. *J. Am. Chem. Soc.* **1996**, *118*, 8329.
- Scolan, E.; Sanchez, C. *Chem. Mater.* **1998**, *10*, 3217.
- Anpo, M.; Shima, T.; Kodama, S.; Kubokawa, Y. *J. Phys. Chem.* **1987**, *91*, 4305.
- Sasaki, T.; Watanabe, M. *J. Am. Chem. Soc.* **1998**, *120*, 4682.
- Gregg, S. J.; Sing, K. S. W. *Adsorption, Surface Area and Porosity*; Academic Press: London, 1982.
- Mikhail, R. S.; Brunauer, S.; Bodor, E. E. *J. Colloid and Interface Sci.* **1968**, *26*, 45.
- Miyoshi, H.; Yoneyama, H. *J. Chem. Soc., Faraday trans. 1* **1989**, *85*, 1873.
- Miyoshi, H.; Mori, H.; Yoneyama, H. *Langmuir* **1991**, *7*, 503.
- Yoneyama, H.; Haga, S.; Yamanaka, S. *J. Phys. Chem.* **1989**, *93*, 4833.
- Enea, O.; Bard, A. J. *J. Phys. Chem.* **1986**, *90*, 301.
- Sato, T.; Okuyama, H.; Endo, T.; Shimada, M. *React. Solids* **1990**, *8*, 63.
- Yanagisawa, M.; Uchida, S.; Fujishiro, Y.; Sato, T. *J. Mater. Chem.* **1998**, *8*, 2835.
- Yanagisawa, M.; Uchida, S.; Yin, S.; Sato, T. *Chem. Mater.* **2001**, *1*, 174.